TOWARDS FAILURE OF CYTOSKELETAL ACTIN NETWORKS

P.R. Onck and E. van der Giessen
Department of Applied Physics, University of Groningen, Nijenborgh 4, 9747 AG Groningen, The Netherlands

ABSTRACT

A numerical model is presented that describes the shear deformation of networks of cross-linked cytoskeletal actin filaments subject to large strains. Thermal undulations are accounted for in the initial configuration. The results show that at small strains the network deforms by filament bending, while at large strains percolations of straightened-out filaments are formed causing severe strain hardening.

1 INTRODUCTION

Living cells have the ability to sense mechanical forces and convert them into a biological reponse. Examples are many sensory functions (including touch, hearing and gravity sensation), tissue growth and healing, bone remodeling, but also fundamental processes like cell growth, cell differentiation and cell death involve specialized mechanotransduction mechanisms. At the same time, genetic programs orchestrate complex cellular processes such as mitosis and cell motility, involving the generation of mechanical forces. The key cellular component that is responsible for the sensing, transmission and generation of mechanical forces is the cytoskeleton.

The cytoskeleton consists of three types of polymer fibers (see Fig. 1), made from different proteins and with different diameters: actin microfilaments (7nm diameter), intermediate filaments (8-12nm) and microtubules (24nm). The structural form in which actin microfilaments appear is mediated by cross-links with actin-binding proteins. Near the cell cortex, actin filaments are usually either forming bundles or a three-dimensional network. Intermediate filaments and microtubules are centrally organized and their organization in the cell is often colinear, spanning the distance between nucleus and cell membrane.

A first step towards understanding the collective behavior of the three different filamental networks making up the cytoskeleton, is to study their behavior in isolation. Janmey and co-workers [1] have studied the viscoelastic behavior of solutions of actin microfilaments, microtubules and intermediate filaments (vimentin), polymerized in vitro. The results show that for the same protein concentration, the actin microfilament network is the stiffest, but ruptures at small strains, after which it behaves like a viscous liquid. The microtubule network has the lowest stiffness, also ruptures, but at much larger strains. Finally, the intermediate filament network has a low stiffness at small strains, but hardens considerably, reaching large stresses and strains without rupturing.

This difference in deformation behavior (at similar protein concentration) can be attributed to the different mechanical properties of the individual protein filaments and to the different three-dimensional architecture of the filament networks resulting from entanglements and cross-links. This work is part of a multiscale cytoskeleton modeling methodology (see Fig. 1). Three size scales are identified: (i) the scale of individual cytoskeletal filaments, (ii) the scale of a network of filaments and (iii) the scale of the cell. The goal is to bridge all size scales involved, from the scale of individual filaments all the way up to the cell scale. The focus of the current paper is on the scale transition of the filament scale to the network scale, directing our attention exclusively on the actin filament network. We will model the deformation behavior of cross-linked actin networks subject to large strains, ultimately leading to failure.

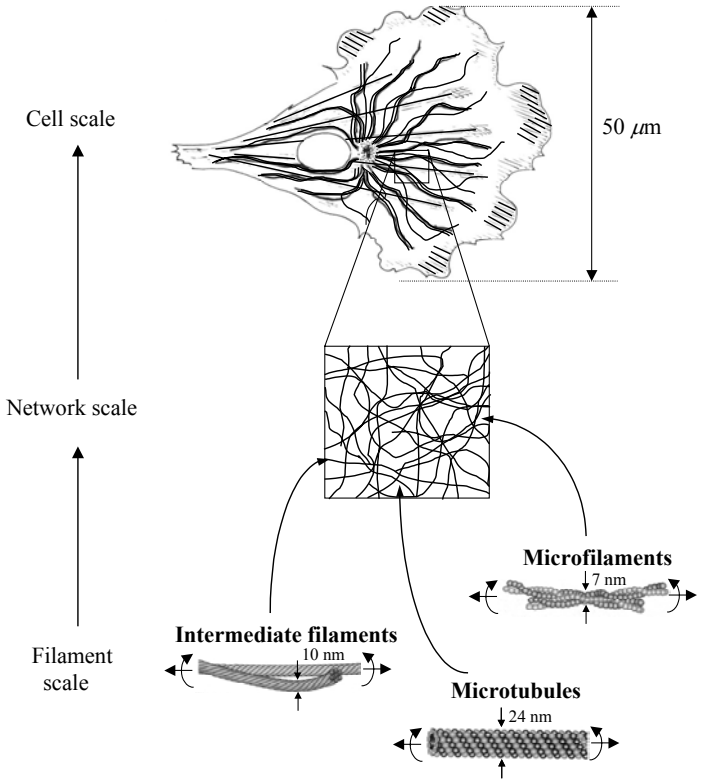

FIGURE 1: Multiscale modeling approach for the cytoskeleton.

2 ACTIN NETWORK MODELING

Isolated actin filaments in solution undergo thermally excited bending motions due to collisions with (water) molecules in the surrounding fluid (see Fig. 2). The resulting deflection v can be described by a superposition of normal modes

$$v(x) = \sum_{n=1}^{\infty} b_n \sin\left(\frac{n\pi x}{L}\right), \tag{1}$$

with b_n the time-dependent amplitude of mode n and L the filament length (see Fig. 2). For small undulations the average bending energy for mode n can be written as

$$\langle U_n \rangle = \left\langle \tfrac{1}{2}\int_0^L EI\left(\frac{\partial^2 v}{\partial x^2}\right)^2 dx \right\rangle = \frac{EIL}{4}\left(\frac{n\pi}{L}\right)^4 \langle b_n^2 \rangle = \frac{EIL}{4}\left(\frac{n\pi}{L}\right)^4 \int_{-\infty}^{\infty} b_n^2 p(b_n)\, db_n, \tag{2}$$

where EI is the bending stiffness of the filament, E Young's modulus and I the moment of inertia. By using Boltzmann's law it follows that $\langle U_n \rangle = k_B T / 2$ and that b_n has a Gaussian distribution with zero mean and a standard deviation given by

$$sd = \sqrt{\frac{2k_B T}{EIL}} \left(\frac{L}{n\pi} \right)^2 = \sqrt{\frac{2}{L_p L}} \left(\frac{L}{n\pi} \right)^2, \tag{3}$$

with the persistence length $L_p = EI / kT$, k_B Boltzmann's constant and T temperature. At low concentrations at finite temperature the filaments in cross-linked actin networks will undergo thermal bending motions which will affect the network's response to deformations applied at low enough rates. Here, we focus on the limit of high strain rates, allowing for thermal motions to be neglected. We do, however, account for thermal undulations in the initial, undeformed network configuration. The initial shape of the filaments follow (1), where we account for the first 10 modes. All filaments are taken to have the same length, L = 10 μm, a Young's modulus E = 2 GPa, and a thickness t = 8 nm (Howard [2]). We perform a two-dimensional analysis assuming all out-of-plane lengths having dimension unity. As a result, the stretching stiffness per unit out-of-plane thickness EA = 16 N/m and the bending stiffness per unit thickness $EI = 8.53 \times 10^{-17}$ Nm. In this two-dimensional setting the persistence length L_p in (3) is scaled to be equal to L (Käs [3]). The position and orientation of the filaments are randomly picked from a uniform distribution. All cross-links between filaments are assumed to be rigid, constraining any relative rotation. We analyze an infinitely wide layer of cross-linked actin filaments, having a height $H = 4L$ (see Fig. 3). The network morphology is assumed to be periodic with period H, so that the analysis can be limited to one unit cell having periodic boundary conditions at the sides. For the numerical study we used the finite element method, discretizing

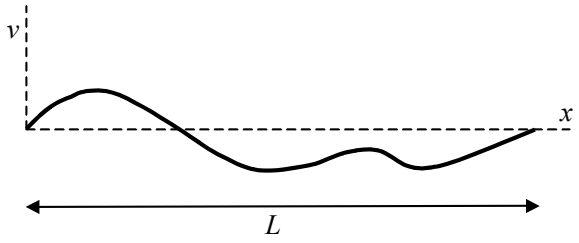

FIGURE 2: Snapshot of an actin filament undergoing thermal fluctuations.

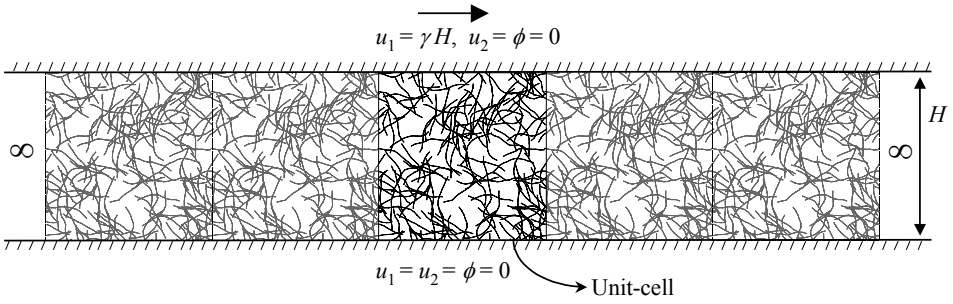

FIGURE 3: Problem definition, consisting of an infinitely wide slab of cross-linked actin filaments subject to shear defromation. Due to periodicity, only the unit-cell of width H is analyzed**.**

each filament with 10 equal-sized Euler-Bernouilli beam elements accounting for stretching and bending. Geometry changes are accounted for by using an updated Lagrangian finite strain analysis. All filaments are perfectly bonded to the top and bottom plates, with the bottom plates fixed and the top plates displaced over a distance $u_1 = \gamma H$, see Fig. 3.

3 RESULTS AND DISCUSSION

We analyze four different concentrations, having relative densities (area covered by filaments divided by total area) of 0.8 %, 1.0 %, 1.2 % and 1.5 %, whose initial configurations are shown in Fig. 4. A shear strain is applied as explained in the previous section and the applied shear stress τ is calculated by adding the total reaction forces (per unit out-of-plane thickness) and dividing by the width H of the unit cell. Figure 5 shows the shear stress-shear strain plots for the four different densities. Figure 5b depicts the full range up to an applied strain of 50 %, while Fig. 5a shows the same results but zoomed-in at the low stress regime. From Fig. 5, three regimes can be identified: (1) a low-stiffness regime; (2) a transition regime and (3) a high-stiffness regime. The stiffnesses

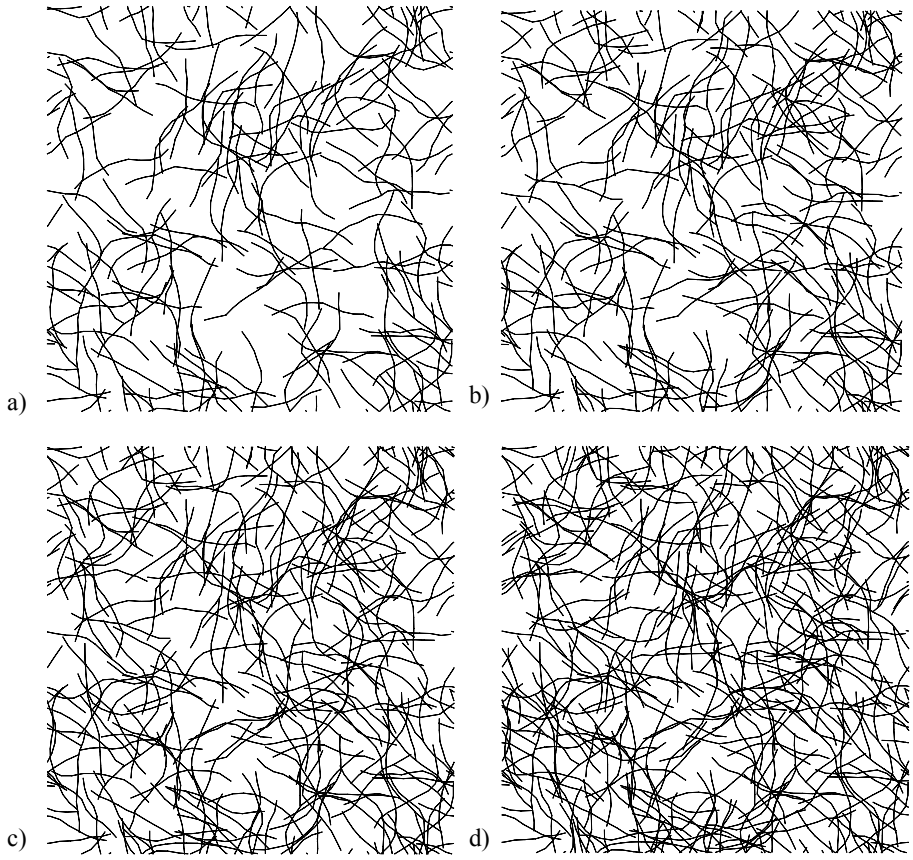

FIGURE 4: Four cases with different relative densities are considered. (a) 0.8 %; (b) 1.0 %; (c) 1.2 %; (d) 1.5 %.

in the regimes 1 and 3 are approximately constant and scale with the density. Figure 6 shows the deformed configurations at two strain levels, $\gamma = 0.125$ and $\gamma = 0.5$, for the relative densities 0.8 % and 1.2 %. In Figs. 6a and 6c ($\gamma = 0.125$) the predominant mode of deformation is bending. This occurs for filaments aligned with the straining direction (at an angle of approximately 45 degrees with respect to the horizontal axis) by pulling out the undulations, for filaments at 90 degrees by bending, orienting them towards the straining direction, and for filaments at 135 degrees by compressive bending ("buckling"), increasing the amplitude of the undulations. Finally, at large strains (Figs. 6b and 6d), percolations of straightened-out filaments are formed that connect the top and bottom plates and are more-or-less aligned with the straining direction. Note that for the low-density network (Fig. 6b) these percolations are one filament thick, while for increasing densities (e.g. Fig. 6d) they appear to form bundles. The filaments in the compressive direction underwent severe compressive loading that has resulted in crumbling.

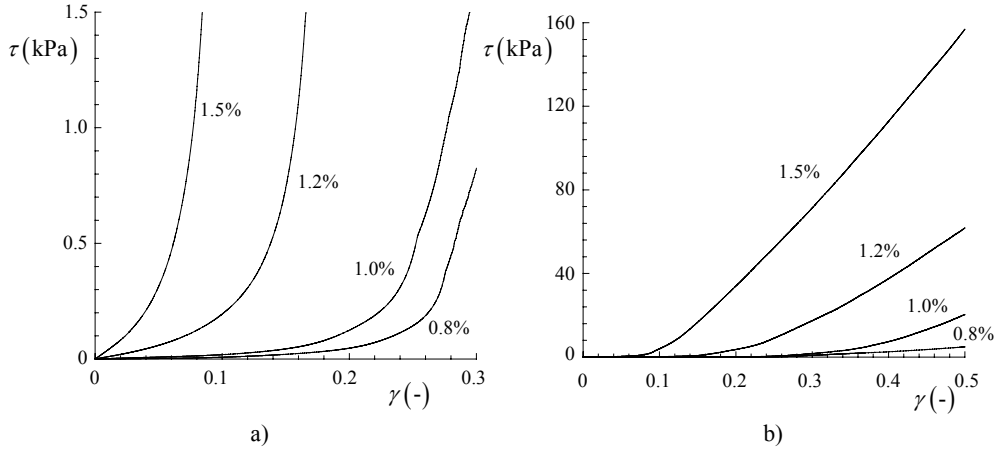

FIGURE 5: Shear stress - shear strain curves for the four different relative densities at (a) low stress range; (b) full range.

4 CONCLUSIONS AND OUTLOOK

The low stiffnesses in regime 1 (Fig. 5) are caused by filament bending. Scaling relations dictate that in this case the stiffness scales with Young's modulus of the filaments multiplied with the relative density to the power 3 (Gibson [4]). The high stiffnesses in regime 3 are caused by the stretching of percolations of straightened-out filaments. The stiffness scales in that case with Young's modulus and the number of percolations, the latter being more numerous at larger densities.

When the percolations are formed at large strains, the tensile forces on the individual filaments and the cross-links are considerable, leading to rupture of the network. Current work is directed towards understanding this rupture behavior, focusing on the dependence of the overall rupture strength and strain on the network architecture and filament and cross-link properties.

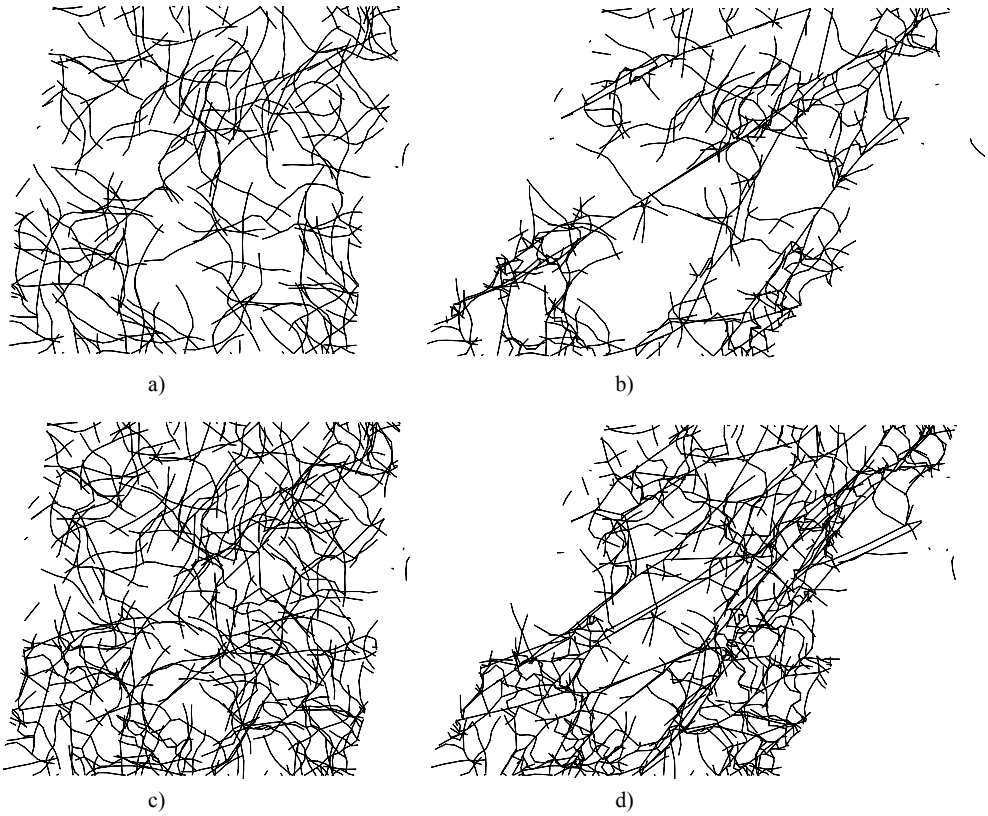

FIGURE 6: Deformed configurations. (a) relative density 0.8 % at $\gamma = 0.125$; (b) relative density 0.8 % at $\gamma = 0.5$; (c) relative density 1.2 % at $\gamma = 0.125$; (b) relative density 1.2 % at $\gamma = 0.5$.

REFERENCES

1. Janmey, P.A., Euteneuer, U., Traub, P. and Schliwa, M., *J. Cell Biol.* vol. 113, 155-160, 1991.
2. Howard, J. *Mechanics of motor proteins and the cytoskeleton*, Sinauer Associates, Inc., Sunderland, Massachusetts, 2001.
3. Kas, J., Strey, H., Tang, J.X., Finger, D., Ezzel, R., Sackmann, E., Janmey, P.A., *Biophys. J.,* vol. 70, 609-625, 1996.
4. Gibson, L.J. and Ashby, M.F. *Cellular Solids,* Cambridge University Press, New York, 1997.